

Non-classical nucleation in supercooled nickel

F. J. Cherne,¹ M. I. Baskes,² R. B. Schwarz,² S. G. Srinivasan,² and W. Klein^{3,4}

¹*Los Alamos National Laboratory
DX-2, Materials Dynamics
Los Alamos, NM 87545*

²*Los Alamos National Laboratory
MST-8 Structure and Property Relations
Los Alamos, NM 87545*

³*Los Alamos National Laboratory
X-7 Material Science
Los Alamos NM 87545*

⁴*Boston University, Department of Physics, Boston, MA 02215
(Dated: June 2, 2018)*

The dynamics of homogeneous nucleation and growth of crystalline nickel from the super-cooled melt is examined during rapid quenching using molecular dynamics and a modified embedded atom method potential. The character of the critical nuclei of the crystallization transition is examined using common neighbor analysis and visualization. At nucleation the saddle point droplet consists of randomly stacked planar structures with an in plane triangular order. These results are consistent with previous theoretical results that predict that the nucleation process in some metals is non-classical due to the presence of long-range forces and a spinodal.

PACS numbers:

INTRODUCTION

Solidification of liquids usually begins by the formation of small clusters or nuclei. Understanding the structure of nuclei and the dynamics of nucleation and growth is of great scientific and technical interest. Nucleation is a highly non-linear process and the interplay between the non-linearity and a change in symmetry is not understood in, for example, the crystallization of super-cooled liquids. In addition to the interesting scientific questions such as the structure of the critical or nucleating droplet and the nature of the initial growth, the form of the nucleation process can have a profound effect on the morphology of the final state. Classical nucleation theories[1] predict that the interior of the critical droplet will have the same structure as the stable phase. However Klein and Leyvraz(KL)[2, 3] have argued that the nucleating droplet in supercooled liquids with long range potentials is non-classical and can have a structure which is significantly different than that of the stable phase due to the presence of a spinodal. They suggest that metals with effective long range interactions due to elastic forces would be a candidate for exhibiting this process which takes place arbitrarily close to a spinodal. The non-classical droplet is predicted to have a density close to that of the supercooled liquid and a triangular structure in 2 dimensions. In 3 dimensions either randomly stacked triangular planes or a bcc structure is predicted depending on the details of the potential. In the initial growth phase of the droplet it is predicted that a core will develop that has the density, and symmetry, of the stable solid phase, or of a metastable solid phase.[3, 4]

Simple models of elastic systems exhibiting an Austen-

ite to Martensite transition have indicated a non-classical nucleation pattern.[5] However, there has been no test of the prediction of non-classical nucleation in either experiment or simulations with realistic metal potentials. Here we present a computational study examining the nucleation and growth in metastable liquid nickel using state-of-the-art semi-empirical potentials. Our results indicate that the nucleation is non-classical and is consistent with nucleation near a spinodal. It is important to stress that by nucleating or critical droplet we refer to the saddle point structure. Physically this is the droplet that just reaches the critical size. This appears in the theory as a saddle point.[3, 6, 7]

METHOD

To perform our simulations we use the modified embedded atom method (MEAM) potential, referred to as potential 4 in Ref. [8]. We extended the radial cutoff, r_{cut} , from 4.0 to 4.8 Å to conserve energy in the liquid phase. This alteration does not affect the solid properties. A thorough discussion of the MEAM formalism can be found in the literature [8, 9, 10] and will not be repeated here. Recently, this particular potential was shown to describe the properties of liquid nickel quite well [11]. The calculated melting point was within 9 % of experiment. The calculated viscosity of 3.84 mPa-s at 1775 K was in agreement with the lower of the experimental range of values ~ 4.0 -6 mPa-s.

We perform a molecular dynamics quenching sequence using an isobaric-isothermal (NPT-ensemble). The MD calculations use a time step of 1 fs. Constant tempera-

ture is maintained by using a Nosé-Hoover [12] thermostat. The Parinello-Rahman method for pressure control is used maintaining the pressure to within ± 100 bar. The sequence is begun by equilibrating a 3D periodic cell of (e.g.) 1500 atoms in the liquid state at a temperature slightly above the melting point of the system for 25 ps. The samples are cooled at 10 K increments and held at that temperature for the length of time corresponding to the desired cooling rate. For example, a 10^{12} K/s cooling rate would be obtained by holding the sample at each temperature step for 10 ps. The quench rates for this study ranged from 10^{11} K/s to 10^{13} K/s. A few calculations are performed using a larger cell of 2048 and 12000 atoms.

Averages of the potential energy and volume are determined at each temperature after 1 ps. The only exception to this is for the quench rate of 10^{13} K/s, where the average temperature and volume are determined for the last 0.5 ps. From this data, we determine whether the specimen is undergoing a liquid-to-crystal or a liquid-to-amorphous transition. The crystallization produces an inflection on the cooling curve and the inflection point determines the solidification temperature, T'_m . The liquid-to-amorphous transition produces a change of slope in the cooling curve. The glass transition temperature, T_g , is determined from the intersection of straight lines fit to the cooling curve above and below T_g .

We use common neighbor analysis (CNA) to identify the local crystalline environment of each atom [13, 14, 15, 16]. This method provides an efficient way to identify the local environment of each atom in the system. The results are quite insensitive to small displacements of the atoms. Since our CNA is not configured to identify planar structures we also perform a visual analysis of possible planar structures both surrounding the 3D Bravais lattice identified by the CNA and free standing (i.e. without the Bravais core).

RESULTS AND DISCUSSION

In Fig. 1, we present the average atomic energies and atomic volumes as a function of temperature for various quench rates. For quench rates below 5×10^{12} K/s a rapid decrease in energy and volume is seen in the region of temperature between 700-900 K. The equilibrium freezing temperature is 1540K[11]. The decrease occurs over a smaller range of temperature as the quench rate is lowered. In contrast, for quench rates of 5×10^{12} K/s and higher (not shown) only a subtle change of slope in the energy or volume is seen. We attribute the rapid decrease in energy and volume to crystallization and the change of slope to solidification into an amorphous state. Below the transition, the curves for both energy and volume are parallel, but offset from each other. Thus the specific heat and thermal expansion of the crystallized material

are independent of quench rate (which determines local structure) but the actual energy and volume differ primarily due to quenched defects (vacancies) in the solid. Above the transition note that the curves all lie on top of each other. The temperature derivative of the liquid energy (specific heat) and volume (thermal expansion) are independent of quench rate. Hence the local structure in the liquid is not affected by the quench rate.

To determine whether there are any important finite size effects we compare the results in systems containing 12000, 2048 and 1500 atoms. The resulting energy curves are shown in Fig. 2. The point where the slope begins to increase as the temperature decreases indicates the onset of crystallization. Nucleation occurs at a slightly higher temperature for a given quench rate as the system size increases. This implies that the system size dependence for nucleation times is as expected[1] and finite size effects are not evident.

Analysis of the resulting microstructure showed that for some conditions the small systems are polycrystalline and others were single crystals. Similarly the large systems exhibit both polycrystalline and single crystalline states. The distribution of the polycrystalline domains is similar in all sizes examined. In addition the CNA as well as visual inspection (to be discussed below) show similar patterns of nucleation. We thus conclude that system size plays no important role in the resulting microstructure.

Using CNA and visual inspection we analyze the nucleation process in supercooled liquid Ni. Upon cooling for both the large system (12,000 atoms) and the small system (1500 atoms), a cluster of atoms having the fcc structure and the hcp structure *appear* to nucleate and grow at approximately $t_o = 1.36$ nanoseconds into the quench. We use *appear* since we are looking for the saddle point object calculated in the theory.[3] After some time into the growth of this cluster the fcc particles dominate the structure. One implication of this result is that the argument of Alexander and McTague[17], does not apply to this particular system[3]. This argument states that in systems where the densities of the liquid and solid are similar the solid phase has a bcc structure. In addition the prediction of icosahedral structures in supercooled liquids as suggested by Frank[18] (Lennard-Jones), Jónsson *et al.*[16] (Lennard-Jones, LJ), and Ramprasad *et al.*[19] (Embedded Atom Method, EAM) is not observed. We attribute these differences to the spherical nature of the LJ and EAM potentials, which do not include angular dependence included in the MEAM potential. This characteristic appears to prevent the formation of icosahedral ordering in pure nickel.

As discussed above, the KL theory [2, 3] predicts stacked triangular planes or bcc for the droplet structure. The KL theory also predicts the development of a classical fcc/hcp core during the growth phase. Therefore we look visually for a halo surrounding the fcc/hcp struc-

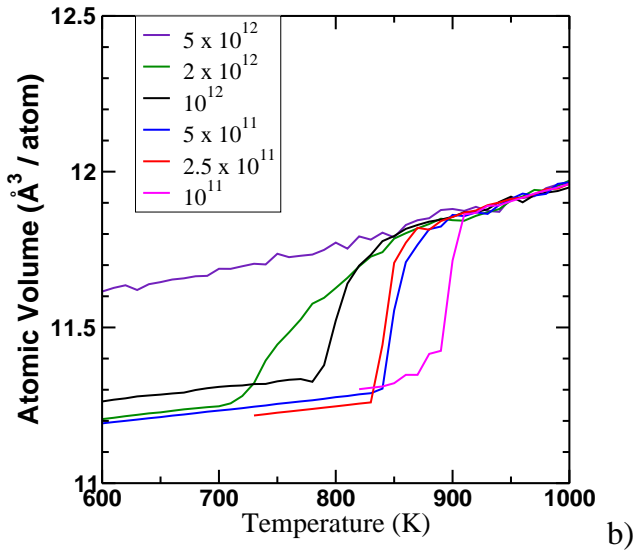
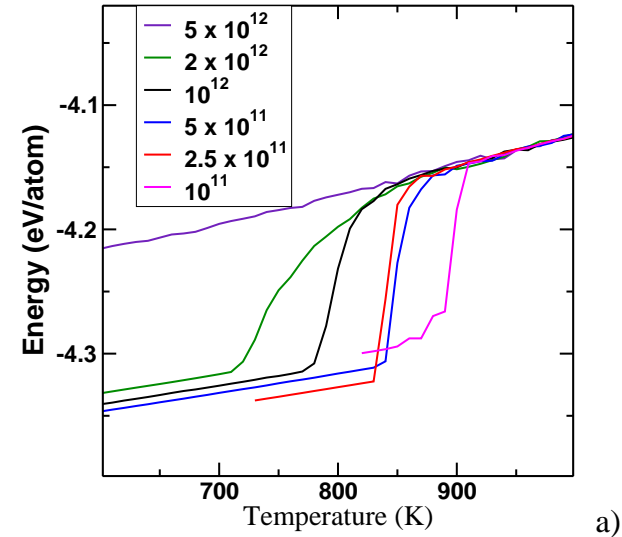


FIG. 1: Figure a) and b) represent the atomic energy and atomic volume as a function of temperature for cooling rates between 10^{11} and 5×10^{12} K/s, respectively.

ture described above. The possibility of a bcc halo was excluded by the CNA analysis so we search for stacked planes with a triangular structure. These were found as illustrated in Fig. 3. We then visually examine the system at 18 ps prior to the configuration at t_o to investigate the possibility that there is a droplet consisting of only stacked triangular planes with no fcc/hcp core. This configuration is also found and is illustrated in Fig. 4.

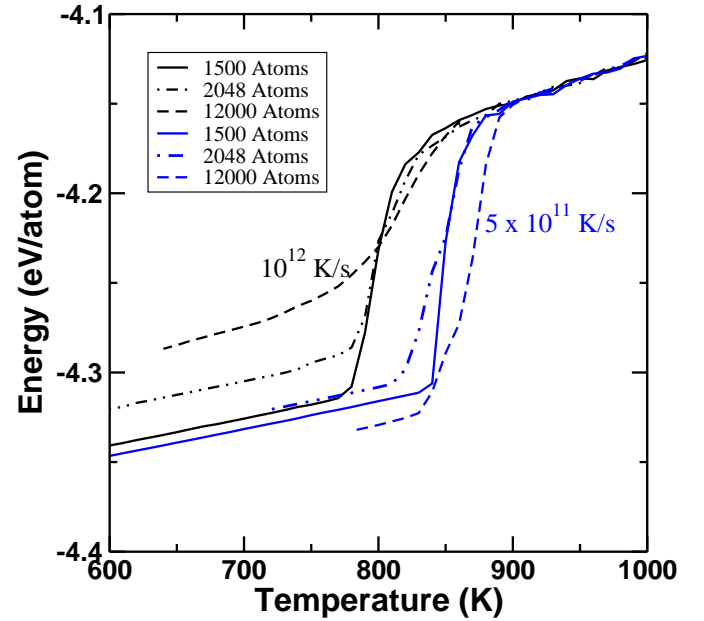


FIG. 2: Comparison between a large system (12000 atoms), a medium system (2048 atoms) and a small system (1500 atoms) of the atomic energy as a function of temperature. The cooling rates shown are 5×10^{11} and 10^{12} K/s. The curves are for a single run.

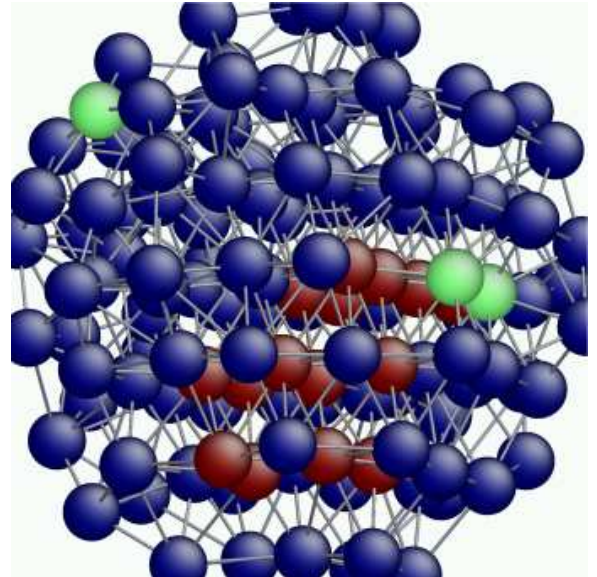


FIG. 3: A 3D representation of the object found at t_o . The droplet consists of an fcc/hcp core surrounded by a halo consisting of planes with an in plane triangular structure. There are 80 atoms in the droplet. The red (green) ball represents an fcc (hcp) atom while the blue balls are in a planar structure.

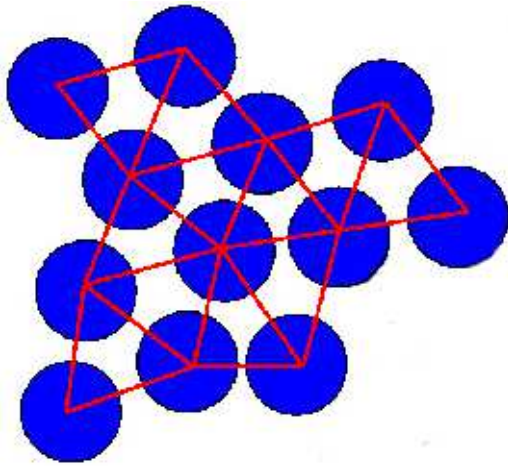


FIG. 4: A 2D representation of one plane in the saddle point droplet. The droplet consists of 4 randomly stacked planes with an in plane triangular order. There are 60 atoms in the droplet

These droplets contain ~ 60 atoms. Finally, we investigate which of these structures; stacked triangular planes with, or without, the core correspond to the saddle point droplet predicted by the theory.[2, 3] This is done via an intervention technique. We take the system at a time which we consider it possible that a nucleation droplet exists in the sense of a saddle point solution. We then make N copies of the system, scramble the velocities keeping the temperature fixed, and then restart each copy. In the $N \rightarrow \infty$ limit a saddle point implies that half of the copies will continue to grow and half will disappear.[20, 21] If the droplet is in the growth phase then $N' \gg N/2$ droplets will grow. If the copies are made prior to the saddle point droplet then $N'' \gg N/2$ droplets will disappear. Using the configuration at $t_o = 1.36$ nanoseconds we find that in all of the copies the droplet grows. We also find that the same result is obtained for configurations chosen at 1.5 and 11.5 ps after t_o . Copies made at 28.5 ps prior to t_o all contain droplets that disappear. However, for configurations chosen at 8.5 and 18.5 ps prior to t_o half of the droplets in the copies disappear and half grow. Since we used $N = 10$ some spread in the location of the saddle point droplet was expected. In addition, the saddle point flattens at the top near a spinodal.[4] Even though there was some spread in the location of the saddle point droplet it is important to note that the droplets at these two times consist only of randomly stacked planes with an in plane triangular structure and do not contain an fcc/hcp core.

In conclusion, our study shows that the local structure of the initial (saddle point) nucleation droplet consists of randomly stacked planes with a triangular ordering. During the initial growth phase a dense core develops which has both fcc and hcp atoms. Further into the growth phase the core becomes dominated by fcc

atoms. This nucleation sequence is in direct contradiction of the argument of Alexander and McTague[3, 17] and appears to exhibit the non-classical behavior that Klein and Leyvraz[2, 3] predicted. This result has important implications for the calculation of nucleation rates and the understanding of the morphology in either the stable or metastable state that has been formed via nucleation. It also gives additional evidence that the spinodal, or limit of metastability of super-cooled liquids may play an important role in determining the local structure of a critical droplet. Finally, non-classical droplets have been found in Lennard-Jones fluids[22, 23] and colloids,[24] however this is the first evidence for non-classical nucleation influenced by a spinodal in a model of a molecular material such as a metal.

-
- [1] J. D. Gunton, M. San-Miguel and P. Sahni in *Phase Transitions and Critical Phenomena* edited by C. Domb and J. L. Lebowitz (Academic, New York, 1983), Vol. 8
 - [2] W. Klein and F. Leyvraz, *Phys. Rev. Lett.* **57**, 2845 (1986).
 - [3] W. Klein, *Phys. Rev. E* **64**, 056110 (2001).
 - [4] C. Unger and W. Klein, *Phys. Rev. B* **31**, 6127 (1985)
 - [5] W. Klein, T. Lookman, A. Saxena and D. Hatch, *Phys. Rev. Lett* **88**, 085701 (2002)
 - [6] J. W. Cahn and J. E. Hilliard, *J. Chem Phys.* **31**, 688 (1959)
 - [7] J. S. Langer, *Annals of Phys.* **41**, 108 (1967)
 - [8] M. I. Baskes, *Mater. Chem. and Phys.* **50**, 152 (1997).
 - [9] M. I. Baskes, *Phys. Rev. B* **46**, 2727 (1992).
 - [10] M.I. Baskes and R.A. Johnson, *Modelling Simul. Mater. Sci. Eng.* **2**, 147 (1994).
 - [11] F.J. Cherne, M.I. Baskes, and P.A. Deymier, *Phys. Rev. B.* **65**, 024209 (2002).
 - [12] S. Nosé, *Prog. Theor. Phys. Suppl.* **103**, 1 (1991).
 - [13] D. Faken, H. Jónsson, *Comp. Mater. Sci.* **2**, 279 (1994).
 - [14] E. Blaisten-Barojas, *Kinam* **6A**, 71 (1984).
 - [15] J. D. Honeycutt and H. C. Andersen, *J. Phys. Chem.* **91**, 4950 (1987).
 - [16] H. Jónsson and H. C. Andersen, *Phys. Rev. Lett.* **60**, 2295 (1988)
 - [17] S. Alexander and J. McTague, *Phys. Rev. Lett.* **41**, 702 (1978).
 - [18] F. C. Frank, *Proc. R. Soc. London, Ser. A.* **215**, 43 (1952).
 - [19] R. Ramprasad and R. G. Hoagland, *Nanophases and Nanocrystalline Materials*, eds. R. D. Shull and J. M. Sanchez, pp. 71-84 (TMS, Warrendale, PA 1993).
 - [20] M. Mandell, J. McTague and A. Rahman, *J. Chem. Phys.* **66**, 3070 (1977)
 - [21] L. Monette and W. Klein, *Phys. Rev. Lett.* **68**, 2336 (1992)
 - [22] J. Yang, H. Gould and W. Klein, *Phy. Rev. Lett.* **60**, 2665 (1988)
 - [23] J. Yang, H. Gould, W. Klein and R. D. Mountain, *J. Chem Phys.***93**, 711 (1990)
 - [24] U. Gasser, E. R. Weeks, A. Schofield, P. N. Pusey and D. A. Weitz, *Science* **292**, 258 (2001)